USING ENGINEERING TOOLS AND NEW PRODUCTS TO PRODUCE THE YATES, QUEEN FORMATIONS IN WARD AND WINKLER COUNTIES

Mike Metza and Pete Wilkinson, Whiting Petroleum Corporation
Dennis Page, Ken Borgen and Robert Reyes, Halliburton

ABSTRACT

Operators have stimulated and produced from the Yates and Queen formation at a depth of 2,500 to 3,100 ft for 77 years. The field was discovered in 1929 and has been explored, developed, bought and sold for many cycles. Each new operator developed the field to different degrees. The typical well produced approximately 4 BOPD and 10 MCFD gas and was stimulated with 75,000 to 100,000 lb of proppant. Operators have been challenged in this field by problems associated with unconsolidated sands while attempting to produce depleted, underpressured intervals. As a booming industry developed, increasing pay zones proved to be economically adequate to produce. Increased activity however exposed a lack of availability of some materials and additives.

To make better wells, new methods and products were developed to reduce formation damage and improve conductivity of the placed frac-pack. To address unconsolidated sand problems, a low-residue, high-yielding guar-based, crosslinked fracturing fluid using a resin-coated proppant was developed. In addition, a new high-yielding liquid gelling concentration was developed that uses less guar to achieve the desired viscosity to minimize formation damage. With resin sand from suppliers becoming scarce to unavailable, a resin-coating additive for proppant was also designed to enable the customer to proceed without having to wait for sand from suppliers. In essence, this resin sand “recipe” enables resin sand to be created on location. In addition, a new modeling tool was used for prefracturing design and for real time operations to model fracture growth geometry. Folds-of-increase curves and Walters & Byrd charts were investigated to determine whether fracture conductivity or fracture length improvement might increase production.

This paper will discuss how this Yates and Queen field was produced using new and improved additives and state-of-the-art engineering tools and techniques to successfully address the operator’s needs.

INTRODUCTION

The Yates and Queen formations in Ward and Winkler counties, Texas, present certain challenges to operators and service providers. The pay rock geology is made primarily of sandstone and dolomites bounded by alternating layers of dolomite and anhydrite with sea level lying between the two formations. The fracture naturally bounds itself with contrasting stress barriers. Pore filling constituents, particularly kaolinite with a very weak bond to pore walls, have a damaging capability to certain treatment fluids; therefore, a 2 to 4% KCl or clay-control substitute based fluid is recommended. To combat damage to the fracture proppant pack and near-fracture face leakoff region, a high-yielding guar was applied to reduce the amount of actual guar used to build the recommended viscosity for the fluid system. The reservoir-produced fluids and high velocity present at the near-wellbore region are detrimental to proppant sand stability. Stabilization occured when these proppant sands were coated to strengthen the proppant pack. A surface modification additive (SMA) was added as a resin-coated sand replacement. Fracture modeling in this field was critical to helping ensure proper design volumes to payzone coverage and conductivity. Logging played an important role with sonic, neutron and density porosity, resisitvity, PE, and calipers used to create parameters for modeling. A well template model was built with these parameters from a computed log. A modeling tool used area-specific equation sets to generate an accurate representation of the downhole environment. Subsquent well models can now be depth-adjusted to the main offset well template. More basic logging tools were then run on all subsequent wells to obtain a well-by-well formation profile accurate to each well. Now, conductivity and effective frac-lengths can be addressed for all wells before stimulation. These fractures and the way they were treated produced multiple fractures with simultaneous extension and fracture overlap. Fold of increase curves, from Walters and Byrd plots, were used to explore how fracture conductivity and effective fracture half-length correlated to production. Fluid testing helped provide a well-to-well assurance. Water analysis, hydration, crosslinking, and break testing was performed to help ensure that fracturing procedures were successful. A working example of Well 1590 was fracture treated and results of a 10-month average production were 11.3 BOPD and 98 Mcf/D.

GEOLOGY

The field has two pay intervals of interest and is located in the Yates and Queen formation. Geological analysis conducted on core samples reveals sandstone and dolomite. The sandstones have average grain size in the range of upper very fine sand (0.095 to 0.108 mm) with the framework grains of these rocks well- to very well-sorted with detrital clay matrix lacking. Most grains have angular or subangular shapes. Point and long grain contacts predominate, with a subordinate number of concavo-convex contacts. Moderate compaction is consistent with these findings. The framework mineralogy is dominated by quartz grains for the sandstone lithology. Subordinate amounts of potassium feldspar, plagioclase feldspar, metamorphic rock fragments, heavy minerals and mica exist as well. Pore filling constituents are authigenic minerals in the sandstone. Detrital clay matrix is uncommon and porosity reduction largely reflects the precipitation of cements. Quartz overgrowths and authigenic clay minerals are the main cementing agents. Minor amounts of dolomite cement, pyrite cement, calcite cement, and organic residue exist. X-ray diffraction analysis of the clay fraction indicates 68–78% kaolinite, 2–4% chlorite, and 0–8% illite/smectite. Pore system properties indicate ratios of 2:1 to nearly 7:1 for primary intergranular pores and secondary leached grain pores. In the sandstone, microporosity contributes to the total measured pore volume, but does little to improve the reservoir potential of the strata. This microspoosity occurs in association with 1) authigenic clay minerals, particularly kaolinite, and 2) partially leached and altered framework grains. The microprosity yields pore systems with high surface area to volume ratios. The lithologic characteristics of these sandstones indicate three principle problems with formation sensitivity: 1) the kaolinite could become dislodged and pose problems with migration fines, 2) the illite may be sensitive to fresh water and undersaturated brines containing monovalent ions, and 3) the iron-bearing minerals, pyrite, iron-rich dolomite (ankerite), and chlorite could react adversely with acids and low pH fluids.

The dolomite pay was deposited with an abundance of carbonate sand grains and relatively little detrital micrite matrix. A combination of coated grains (ooids and oncoids), peloids, and skeletal grains are present. The texture and grain types in this rock are consistent with sedimentation in a moderate to high energy, shallow subtidal shoal setting. The pore system of this dolomite is complex, consisting of three principal components: 1) 13% from intergranular pores between the framework grains, 2) 33% moldic pores from partial or complete dissolution of framework grains, and 3) 48% small intercrystalline pores and micropores. The remainder consists of 6% indeterminate pores and other pore types. The moldic pores and small intercrystalline pores/micropores developed due to diagenetic alterations of the rock, whereas, the intergranular pores are relict primary pores. The moldic pores and intercrystalline microporosity may be rather ineffective components of the pore network; that is, these secondary pores may account for the high porosity (20%), but relatively low permeability (2.97md) determined for this dolostone.

HIGH-YIELDING GUAR TECHNOLOGY

Damage resulting from hydraulic fracturing takes two distinct forms: 1) damage inside the fracture itself (proppant-pack damage), and 2) damage normal to the fracture intruding into the reservoir (fracture-face damage). The first form of damage generally occurs because of inadequate breaking of the fracturing-fluid polymer; the second occurs because of excess leakoff.[1] The damage can occur from residue guar that stays in the permeability of the rock matrix and proppant pack (see **Figure 1**). A high-yielding liquid gelling concentration has been researched and designed. This new liquid gelling agent was developed for use in coalbed methane (CBM) fracture-stimulation applications. One feature of this gelling agent is that less guar is used to achieve the desired viscosity than in previous gelling systems. The use of less guar results in less formation damage.

CONDUCTIVITY-ENDURANCE FRACTURING TECHNOLOGY

Recent research has demonstrated and field results have proved that conductivity-endurance fracturing can enhance the outcome of stimulation treatments and achieve sustained production increases through a combination of factors, including: (1) proper treatment design, (2) low-damaging fluid systems, (3) accurate proppant selection, and (4) coating and propping materials.[2]

Within the industry, several conductivity-enhancing mechanisms have been suggested. Two important mechanisms resulting from increased surface tackiness are: increased proppant pack porosity resulting in increased pack permeability; and increased proppant pack stability that prevents encroachment of formation fines into the pack and migration of fines within the proppant pack.[3]

Studies indicate that as little as 25% of the initial proppant-pack porosity may remain after only 40 days at 300°F and 6,000-psi closure stress. The rate of porosity loss can be influenced by the surface treatment of the proppant, which indicates that some control of this process may be accomplished. The use of surface-modification agents (SMA) to coat proppants used in propping hydraulic fractures resulted in sustained and more uniform production from wells.[4]

A new proppant-consolidating treatment, or SMA, has been developed to remedy the flowback of unconsolidated proppant. Because of problems with availability of resin proppants, a new method of delivering resin-coated proppant to the producer has also been developed. The treatment is a two-component, proppant-consolidation system. It is an epoxy-based resin system that coats the proppant during treatment of the well and allows superior proppant flowback control to help provide higher producing wells. The treatment chemical has a delayed cure to allow for cleanout in the event of a screenout. The delayed cure also allows the chemical to be pulled into grain-to-grain contact points by capillary pressure, which results in a higher-strength proppant pack. Therefore the proppant-consolidating treatment can withstand higher stress and sustain better conductivity than other coated proppants. The consolidation strength occurs quickly, reducing the amount of proppant flowback during the cleanup process and production of the well. **Figure 2** compares the conductivity of treatment-coated sand and resin-coated sand. The treatment-coated sand has as much as three times more conductivity than the resin-coated sand.

PROPPANT-CONSOLIDATING TREATMENT APPLICATION

The new resin system is comprised of two components: a resin and a hardener. The resin and hardener are delivered to location in separate totes and pumped at a 1:1 ratio through a static mixer, which creates a homogeneous blend. The blend is then dry-coated through the sand screws onto the proppant as the proppant moves to the blender tub and is then pumped downhole. Downhole in the fracture, the gelled carrying fluid should break first, allowing the proppant to obtain grain-to-grain contact; reservoir temperature will then cause the resin to cure. The proppant pack will form a solid consolidated mass. The temperature range for the new treatment is 60 to 225°F. The well should be shut in for the recommended time to allow the resin to cure. All rigup and pump procedures concerning the consolidation treatment should be predetermined before the job.

LOGGING RESPONSE

Figure 3 shows a computed log that uses logging responses to calculate desired parameters. The parameters required by the modeling software are lithology, water saturation, porosity, permeability, Poisson's ratio, Young's modulus, and stress (each will be discussed in a later section). Equation sets have been formulated to compute these values using certain area constants.

To compute lithology, a volume of shale must be calculated from either Clavier or Steiber equations. These are

$$Vshclav = 1.7 - ((3.38 - (GRI + 0.7)^2))^{1/2} \qquad \text{(Eq. 1)}$$

$$Vshsteib = (0.5 * GRI) / (1.5 - GRI) \qquad \text{(Eq. 2)}$$

Gamma ray index is

$$GRI = (GR / GRcln) / (GRsh - GRcln) \qquad \text{(Eq. 3)}$$

To compute effective water saturation, Sw, a cementation constant C is used for lithology, resistivity of water Rw, porosity corrected for oil or gas PHIeff, and resistivity reading HDRS.

$$Sweff = \frac{(C * Rw/PHIeff^2) * ((5 * PHIeff^2)}{Rw * HDRS + (Vsh/Rshl)^2)^{1/2} - (Vsh/Rsh)} \qquad \text{(Eq. 4)}$$

$$PHIeff = (NPHIeff + DPHIeff) / 2 \quad \text{for oil.} \qquad \text{(Eq. 5)}$$

$$PHIeff = (NPHIeff^2 + DPHIeff^2) / 2 \quad \text{for gas.} \qquad \text{(Eq. 6)}$$

$$NPHIeff = NPHI - (Vsh * PHIncrossplot) \qquad \text{(Eq. 7)}$$

$$DPHIeff = DPHI - (Vsh * PHIdcrossplot) \quad \text{(Eq. 8)}$$

If cores are cut, then

$$DPHI = (RhoM - RhoB) / (RhoM - RhoF) \quad \text{(Eq. 9)}$$

RhoM is density from core

RhoB is bulk density

RhoF is density from water

Young's modulus is first calculated dynamic

$$E = \frac{(13474 * RhoB / DTS^2) * ((3 * (DTS/DTC)^2 - 4)}{((DTS/DTC)^2 - 1)} \quad \text{(Eq. 10)}$$

Then must be converted to static using either

$$Em = (10^{(A1 + A2 * \log (E * 1000000))}) / 1000000 \quad \text{by moroles} \quad \text{(Eq. 11)}$$

$$Ep = (0.8 - DPHI) * E \quad \text{by porosity} \quad \text{(Eq. 12)}$$

Poisson's ratio is computed by

$$V = \frac{V = ((DTS / DTC)^2 - 2)}{(2 * (DTS / DTC)^2 - 2)} \quad \text{(Eq. 13)}$$

Irreducible water saturation by

$$Sw = (C1 * PHIeff^{C2}) \quad \text{(Eq. 14)}$$

Now absolute permeability by

$$K = ((100 * PHIeff/CC)^2 * (FFI / BVI))^2 \quad \text{(Eq. 15)}$$

Where, $FFI = PHIeff - BVI$

And $BVI = Sw * PHIeff$.

Finally, effective permeability by

$$Khc = K * ((0.97 - Sweff) / (0.97 - Sw))^{3.2} \quad \text{for hydrocarbon} \quad \text{(Eq. 16)}$$

$$Kw = K * ((Sweff - Sw) / (1 - Sw))^{3.6} \quad \text{for water} \quad \text{(Eq. 17)}$$

The log must first be layered for lithology and formations. A direct method for labeling lithology would be to use a photo-electric factor logging tool. When this is not available, the gamma ray index is calculated and applied. By picking high and low gamma ray readings for sand and shale using Eq. 3, a gamma index is calculated. Volume of shale can be calculated by Clavier or Steiber (Eqs. 1 and 2 respectively). A value can be assigned to the volume of shale and gamma index to label lithology accordingly.

Porosity, or void in the rock, can be calculated two ways. The effective porosity takes into account the volume of shale to give a more accurate value than merely reading a neutron and density crossplot porosity. This is done as Eq. 5 or 6. Porosity by cores is calculated using Eq. 9. Bulk density from logging must be known for this method.

Youngs modulus, or the stiffness of the rock, can be calculated using Eq. 10 if shear and compressional wave train data is available. This value is from dynamic readings and must be converted to static by Eq. 11 or 12. Area constants dictate which formula and constants to use.

Poison's ratio, the stress-to-strain ratio, is calculated using sonic logging data and Eq. 13.

Absolute permeability is calculated using Eq. 15. Absolute permeability takes into account bulk volume index and free-flowing water. To obtain effective permeability, discount for irreducible water saturation (Eq. 14) and effective water saturation for volume of shale present using Eq. 4. Effective permeability is calculated using Eq. 16 for hydrocarbon and Eq. 17 for water.

MODELING TOOLS

Fracture models are used as a tool to predict geometry and production. Most of today's models came from the same origins. All early models were developed to calculate fracture geometry for a given rate and length but a volume balance was not built into these programs. Khrishianovich,[5] whose model simplified fluid flow and concentrated on solids mechanics attempted to predict fracture width. Carter[6] developed a model to satisfy a volume balance and leakoff but neglected fluid viscosity and solid mechanics and assumed a constant width. This was the model used for the mass volume balance while Khristianovich's model was used to predict width until the 1970s when better models were needed to predict width for proppant placement. Two models surfaced, PKN and KDG (see **Figure 4**), which were made to address solids mechanics for predicting width and included a volume balance. PKN and KDG both were applicable for fully confined fracture environments predicting high net pressures and longer fractures and differed in the way they converted 3D solids and fracture mechanics into a 2D plain-strain model. PKN assumed that the vertical cross-section acts independently. Pressure at any section is dominated by height of the section rather than length of the fracture. KDG assumed plane strain in the horizontal direction. All horizontal cross-sections act independently. Fracture width changes slower vertically along the fracture face than it does horizontally.

Modeling how fast the fluid leaks off into the formation is a key issue in the fracture treatment. Three time periods for fracture fluid leakoff must be looked at to accurately predict fracture geometry.[7] During the initial period, leakoff is quick and a filter cake has not been formed; therefore, leakoff is controlled by the resistance of the formation to flow of the fracture fluid. Then follows a decreasing leakoff rate where an external filter cake builds, which stops developing thickness because the high-velocity fluid in the fracture prevents further polymer deposition. These first two periods of leakoff contribute in volume to a quantity called spurt volume. The last stage is referred to as dynamic leakoff.

Fluid loss drives the pressure drop for three individual loss mechanisms. These are filter cake,

$$Cw = ((\, Kcake\ \alpha\ \Delta Pcake) / 2\mu filtrate\,)^{1/2}. \qquad \text{(Eq. 18)}$$

Which assumes rate of filtration is proportional to square root of time, amount of cake deposited is proportional to the volume of fluid (Vl) passed through a unit surface area, cake permeability (Kcake) is independent of its thickness, fls through the cake obeys Darcy's law, and pressure drop across cake (ΔPcake) is constant.

And filtrate zone,

$$Cv = ((\, Kfiltrate\ \varphi\ \Delta Pv) / 2\mu filtrate\,)^{1/2}. \qquad \text{(Eq. 19)}$$

Which assumes pressure drop (ΔPv) across the zone is constant, filtrate fully displaces the mobile phase within the formation (piston-like displacement, 100% filtrate saturation), and the fluid and rock are incompressible.

And reservoir zone,

$$Cc = (\, Kr\ Ct\ \varphi / \Pi \mu r)^{1/2}\ \Delta Pc. \qquad \text{(Eq. 20)}$$

Which assumes a constant pressure drop between the filtrate and reservoir interface and the far-field reservoir, compressible fluid, constant total compressibility (Ct), relatively slow movement of the front of the invading fluid, and infinite reservoir.

To sum up leakoff in actual practice, Ct is the total leakoff and is the summation of all three processes, which occur simultaneously.

$$Ct = ((Kcake\ \alpha\ \Delta Pcake) / 2\mu filtrate)^{1/2} + \qquad \text{(Eq. 21)}$$

$$((Kfiltrate\ \varphi\ \Delta Pv) / 2\mu filtrate)^{1/2} +$$

$$(Kr\ Ct\ \varphi / \Pi\mu r)^{1/2}\ \Delta Pc. =$$

$$Cw + Cv + Cc$$

A fracture modeling tool was used to determine fracture geometry and conductivity numbers for an in-place proppant pack. Logging response was used to input into the modeling tool. Well spacing, net pay footage and formation permeability are the main drainage parameters that dictate the type of fracture to design for. In the software model for these fields, four to eight fractures initiated and established extension. The well, GWO 1590 (as example), established the geometry seen in **Table 1**, which shows effective fracture length and conductivity for seven fractures. Using desired parameters of 150- to 125-ft fracture lengths and height containment as design givens, a model was built. From the results in the log, the formation layer properties in **Table 2** were populated. Values generated earlier, such as stress, Young's modulus, Poisson's ratio, and permeability were used for the tool to generate a downhole formation model. A pumping schedule (**Tables 3** and **4**) is also incorporated in the model. The fracture profile, or output, is shown on **Figures 5 and 6** for the Yates and Queen formations respectively.

WALTERS AND BYRD

A Walters and Byrd chart was used to determine a fold-of-increase starting point after this design and treatment. This starting point can be used to see what kind of folds of increase improvement would be possible with an alternate treatment design. With 10-acre spacing, a net pay of 100 feet, and permeability of 3 md in the pay sandstones, a fracture with 150- to 200-ft half-length was the criteria and folds of increase were plotted. The Walters and Byrd chart is shown in Figure 4 with values plotted (refer to Table 1, green colored plots are for the Queen fracture treatment while red plotted values are for the Yates fracture treatment). From the location of these plots, it is evident that an increase in fracture conductivity will result in more folds of increase in some of the fractures. A fold-of-increase improvement should result in a greater produced hydrocarbon rate from the well if the reservoir is prolific enough to yield higher hydrocarbon rates. In Eq. 22, the proppant pack conductivity numerator portion of the fraction must be increased or the formation conductivity denominator must be decreased. In this formation, it was desirable to have as much fracture length as economically possible if the reservoir permeability was a given. Therefore, to improve the fracture conductivity, Y-intercept, the proppant pack conductivity should be addressed not the formation conductivity. Reducing the width would jeopardize the fracture design being placed and increasing it would be limited. The logical choice for improving the fracture conductivity was to improve the proppant pack permeability. Improving the proppant pack conductivity is accomplished by using a larger proppant mesh, coating the proppant, or both, to achieve better proppant pack conductivity values. (Addressing proppant pack conductivity by coating the entire proppant pumped is a recommended topic for a future study). A mesh change was made when 12/20 proppant was replaced with 8/16 proppant. Using 8/16 proppant will increase proppant pack conductivity and more evaluation will determine whether this change correlates to an increased hydrocarbon rate (another topic for future work). For this study, the actual design using modeling tools and improved additives is the frame of discussion.

$$Fcd = (Kf * Wf) / (K * Lf) \qquad \text{(Eq. 22)}$$

Kf – fracture permeability

Wf – propped fracture width

K – reservoir permeability

Lf – propped fracture length

FLUIDS LAB WORK

Fracturing a formation at a certain depth hydraulically and placing a desired concentration of proppant in the created fracture requires, among many things, a fluid system with predetermined expectations. The performance of the fluid system should be fine-tuned during laboratory testing. The proppant-consolidating treatment was used for this treatment and is expected to be free of bacteria, hydrate to a predetermined viscosity, crosslink, remain stable for a given time, then break back to a viscosity of water. These items are determined by testing before every fracturing procedure. Because the friction pressure for fluid traveling down the wellbore tubulars was low, an instant crosslinker was chosen. Job design history and modern modeling indicate that in the Yates formation, placing 8/16-mesh Brown sand at a depth of 2,800 to 3000 feet, creating 100 to 175 feet of length requires 3,000 horsepower to obtain adequate pump rate and volumes. A pumping schedule requiring a 45-minute pump time with a quick flowback schedule defines the fluid to be "broke" or have a viscosity of below 10 cp in 1 to 1 1/2 hours. It is recommended to shut in the well after treatment to allow the flowback-control coating to cure, but a quicker flowback was sought by the operator and historical background for this field indicated that flowing the well back immediately would not negatively affect this formation or the placed proppant pack. Lab results for the job are shown in **Figures 7**, **8**, and **9.**

METHODOLOGY OF STIMULATING WELLS

A typical treatment designed with modeling software is shown in Tables 3 and 4. Here a pad volume of approximately 30% is used to place 75,000 to 100,000 lbm of 12/20-mesh Brady sand with proppant flowback-control coating the last 3,000 to 4,000 gallons of sand-laden fluid. Later modeling showed that switching 12/20-mesh Brady sand to 8/16-mesh Brady sand would benefit production by producing a higher conductivity proppant pack. This mesh also was more easily available from sand suppliers, but unfortunately, is also more punishing to pumping units. The treatment is flushed just short of the top perforation and flowed back as soon as the pumping crew is rigged off location and out of the way of the wellhead. This treatment is designed to achieve 150 to 250 feet of effective fracture length. A typical treatment data plot is shown in **Figure 10** with the required additives shown on **Figure 11**. In the additive chart (Figure 14), the two proppant flowback-control components pumped in the last 3-lbm/gal sand concentration holding stage can be observed and shown as Item 5 on the chart. The instantaneous shut-in pressure (ISIP) was taken when pump rates stopped at 10:40 on the treatment data on Figure 14. The ISIP is used to calculate a stress gradient. This gradient is used in modeling software to calibrate stress at fracture depth with the minimum stress that exists downhole.

As the minimum stress approaches overburden at this depth the fracture plane is no longer a true vertical plane. The fractures will start turning on the preferred plane leaning more toward horizontal. The fractures can actually overlap one another in this stress environment and each fracture width can start to compete with others. The two formations, Queen and Yates, generated seven fractures in this case. The fractures were 284, 283, and 279 feet on the Queen and 126, 171, 152, and 247 feet on the Yates (see Figures 5 and 6, fracture profiles for these fracture half-lengths). These fractures correspond with conductivities of 997, 3506, and 0 md-ft respectively for the Queen and 5066, 4385, 2274, and 209 md-ft respectively for the Yates. Plotting these on Walters and Byrd production increase curves **Figure 12** reveals that three fractures will have no increase in production as a result of increasing fracture conductivity. However, four of the fractures show that an increase in production will result if more fracture conductivity can be achieved. Eq. 22 shows that by increasing the numerator in the equation, the dimensionless conductivity factor will increase. The dimensionless conductivity factor could be improved by designing for a proppant with better conductivity numbers, which will be the subject for a future study. Possibly, an attempt can be made to improve the conductivity of the in-place proppant.

Field Procedure: Job Example for Well GWO 1590

1. Stage 1: Fracture the Queen interval (3,109–3,390 feet) with 49,000 gal of crosslinked proppant-consolidating treatment carrying 81,800 lb of 12/20-mesh premium Brown sand. Sand pumped during the final 3-lbm/gal sand stage (Stage 5) will be coated with 1.5% proppant flowback-control fluid. Treat via 5 1/2-in. casing at 35 bbl/min with an anticipated wellhead treating pressure (WHTP) of 1,800 psi. Use the schedule shown in Table 2.

2. Run in hole with wireline-set bridge plug and set at ± 3,050 ft.

3. Perforate the Yates interval (2,612–2,849 ft) and prepare to frac.

4. Stage 2: Fracture the Yates interval (2,612–2,849 ft) with 54,000 gal of crosslinked proppant-consolidating treatment carrying 81,800 lb of 12/20-mesh premium Brown sand. Sand pumped during the final 3-lbm/gal sand stage (Stage 5) will be coated with 1.5% proppant flowback-control fluid. Treat via 5 1/2-in. casing at 35 bbl/min with an anticipated WHTP of 1,500 psi. Use the schedule shown in Table 3.

SUMMARY

Production after this program showed an average increase from 4 BOPD, 110 BWPD, and 10 Mcf/D to 20 BOPD, 230 BWPD, and 30 Mcf/D. In summary, the operator accomplished greater production in the Queen and Yates fields of Ward and Winkler counties. This was made possible through use of the processes, engineering tools, and new additives used in this program.

Although liquid gelling agents have been around for many years, a new higher-yielding liquid gel system was employed to establish the desired viscosity while using a lower gel loading to do so. The average gel loading was reduced from 6.25 to 5 gal/Mgal using the new proppant-consolidating treatment to produce a 16 viscosity system. This is equivalent to a 25-lb/gal base fluid.

To combat the flowback of unconsolidated proppant, the operator required a resin-coated proppant. The service company delivered a SMA to consolidate the proppant pack while obtaining a high proppant-pack conductivity. In turn, these two mechanisms mitigated fracture damage and resulted in better wells.

The service company also designed the fracturing procedures for this program using engineering modeling tools to achieve better pay zone coverage by maximizing fracture height and length while sustaining conductivity. Post-job pressure matching calibrated the model.

Lastly, by using Walters and Byrd folds of increase charts, it is observed that folds of increase are possible if fracture conductivity can be improved. This phenomenon is based on tool response, although sometimes tools or models may not be precise. Both careful consideration and sound engineering experience was applied when making adjustments to the actual design. Engineering principles were used to design the program based on what was known to indicate where work should be directed to improve output. It may be possible to improve hydrocarbon production even more in these fields by coating the entire proppant pumped with proppant flowback-control fluid. This type of change to the design would significantly increase design cost and would then need to be evaluated carefully to determine whether the change would be cost-effective for the operator's and service company's efforts. Other service company case histories (from other formations and areas) show that making such a change has increased production.

REFERENCES

1. Economides, M.J. and Nolte, K.G., Eds. Reservoir Stimulation, Third Ed., John Wiley & Sons, (2000).
2. Barree, B., *et al*.: "Propping Up Production," *Conductivity Endurance*, Special Publication, E&P and Oil and Gas Investor and Halliburton, Hart Energy Publishing.
3. "Stick to Tacky. It Pays." *Conductivity Endurance*, Special Publication, E&P and Oil and Gas Investor and Halliburton, Hart Energy Publishing.
4. Weaver, J., *et al*.: "Sustaining Conductivity," paper SPE 98236 presented at the 2006 International Symposium and Exhibit on Formation Damage Control, Lafayette, Louisiana, 15-17 February.
5. Khrishianovich, *Conductivity Endurance*, Special Publication, E&P and Oil and Gas Investor and Halliburton, Hart Energy Publishing (1955).
6. Carter, *Conductivity Endurance*, Special Publication, E&P and Oil and Gas Investor and Halliburton, Hart Energy Publishing (1957).
7. Williams, *Conductivity Endurance*, Special Publication, E&P and Oil and Gas Investor and Halliburton, Hart Energy Publishing (1970).

Table 1
Frac Dimensions from Log

Queen Formation, green star		Yates Formation, red star	
Frac Length	**Conductivity**	**Frac Length**	**Conductivity**
284	977	126	5066
283	3506	171	4385
279	0	152	2274
		247	209

Table 2
Formation Layer Properties

	Depth TVD (ft)	Depth MD (ft)	Layer Thickness (ft)	Rock Type	Stress (psi)	Young's Modulus (psi)	Poisson's Ratio	Fracture Toughness (psi·in½)	Composite Layering Effect	Est Ht/Len Growth	Pore Fluid Permeability (mD)	Leakoff Coefficient (ft/min½)	Pay Zone
16	1,880.0	1,880.0	50.0	Sandstone	1,300	2.86E+06	0.308	0.0	0.00	0.00	0.0000E+00	0.0000E+00	
17	1,930.0	1,930.0	10.0	Anhydrite	1,646	4.88E+06	0.312	0.0	0.00	0.00	5.0000E-02	1.1268E-03	
18	1,940.0	1,940.0	50.0	Limestone	1,391	3.11E+06	0.322	0.0	0.00	0.00	5.0000E-01	3.0434E-03	
19	1,990.0	1,990.0	180.0	Anhydrite	1,717	4.75E+06	0.316	0.0	0.00	0.00	5.0000E-02	1.1268E-03	
20	2,170.0	2,170.0	180.0	Sandstone	1,480	2.45E+06	0.286	0.0	0.00	0.00	1.0000E-02	5.1247E-04	
21	2,350.0	2,350.0	150.0	Anhydrite	1,805	5.51E+06	0.318	0.0	0.00	0.00	5.0000E-02	1.1268E-03	
22	2,500.0	2,500.0	35.0	Sandstone	1,803	1.96E+06	0.338	0.0	0.00	0.00	5.0000E-01	3.0434E-03	
23	2,535.0	2,535.0	55.0	Dolomite	1,720	2.67E+06	0.326	0.0	0.00	0.00	5.0000E-01	3.0434E-03	
24	2,590.0	2,590.0	35.0	Sandstone	1,968	1.35E+06	0.361	0.0	0.00	0.00	5.0000E-01	3.0434E-03	✓
25	2,625.0	2,625.0	5.0	Dolomite	1,632	3.94E+06	0.321	0.0	0.00	0.00	5.0000E-01	3.0434E-03	✓
26	2,630.0	2,630.0	25.0	Sandstone	1,774	2.59E+06	0.329	0.0	0.00	0.00	5.0000E-01	3.0434E-03	✓
27	2,655.0	2,655.0	10.0	Dolomite	1,572	5.01E+06	0.322	0.0	0.00	0.00	5.0000E-01	3.0434E-03	✓
28	2,665.0	2,665.0	50.0	Sandstone	1,748	3.02E+06	0.322	0.0	0.00	0.00	5.0000E-01	3.0434E-03	
29	2,715.0	2,715.0	15.0	Dolomite	1,677	4.62E+06	0.311	0.0	0.00	0.00	5.0000E-01	3.0434E-03	
30	2,730.0	2,730.0	20.0	Sandstone	1,789	2.72E+06	0.312	0.0	0.00	0.00	5.0000E-02	1.1268E-03	
31	2,750.0	2,750.0	10.0	Dolomite	1,643	4.85E+06	0.309	0.0	0.00	0.00	5.0000E-02	1.1268E-03	
32	2,760.0	2,760.0	10.0	Sandstone	1,914	2.37E+06	0.325	0.0	0.00	0.00	5.0000E-02	1.1268E-03	
33	2,770.0	2,770.0	5.0	Dolomite	1,633	5.58E+06	0.315	0.0	0.00	0.00	5.0000E-02	1.1268E-03	
34	2,775.0	2,775.0	5.0	Dolomite	1,716	5.79E+06	0.313	0.0	0.00	0.00	5.0000E-02	1.1268E-03	
35	2,780.0	2,780.0	30.0	Sandstone	1,812	3.83E+06	0.308	0.0	0.00	0.00	5.0000E-02	1.1268E-03	
36	2,810.0	2,810.0	20.0	Dolomite	1,787	5.21E+06	0.316	0.0	0.00	0.00	0.0000E+00	0.0000E+00	
37	2,830.0	2,830.0	25.0	Sandstone	1,893	3.01E+06	0.299	0.0	0.00	0.00	0.0000E+00	0.0000E+00	
38	2,855.0	2,855.0	160.0	Dolomite	1,663	6.37E+06	0.313	0.0	0.00	0.00	0.0000E+00	0.0000E+00	
39	3,015.0	3,015.0	35.0	Sandstone	1,767	4.72E+06	0.300	0.0	0.00	0.00	0.0000E+00	0.0000E+00	
40	3,050.0	3,050.0	10.0	Dolomite	1,752	5.96E+06	0.311	0.0	0.00	0.00	0.0000E+00	0.0000E+00	
41	3,060.0	3,060.0	10.0	Sandstone	2,046	2.98E+06	0.322	0.0	0.00	0.00	0.0000E+00	0.0000E+00	✓
42	3,070.0	3,070.0	30.0	Dolomite	1,842	5.30E+06	0.321	0.0	0.00	0.00	1.0000E-02	5.1247E-04	
43	3,100.0	3,100.0	20.0	Sandstone	1,814	4.84E+06	0.296	0.0	0.00	0.00	1.0000E-02	5.1247E-04	✓
44	3,120.0	3,120.0	20.0	Sandstone	1,824	4.32E+06	0.290	0.0	0.00	0.00	1.0000E-02	5.1247E-04	✓
45	3,140.0	3,140.0	25.0	Sandstone	1,839	4.10E+06	0.283	0.0	0.00	0.00	1.0000E-02	5.1247E-04	✓
46	3,165.0	3,165.0	10.0	Dolomite	1,788	5.59E+06	0.303	0.0	0.00	0.00	1.0000E-02	5.1247E-04	
47	3,175.0	3,175.0	10.0	Sandstone	1,911	3.63E+06	0.283	0.0	0.00	0.00	5.0000E-01	3.0434E-03	✓
48	3,185.0	3,185.0	10.0	Dolomite	1,896	5.15E+06	0.308	0.0	0.00	0.00	5.0000E-01	3.0434E-03	
49	3,195.0	3,195.0	10.0	Sandstone	1,911	3.63E+06	0.283	0.0	0.00	0.00	5.0000E-01	3.0434E-03	
50	3,205.0	3,205.0	5.0	Dolomite	2,012	4.37E+06	0.314	0.0	0.00	0.00	5.0000E-01	3.0434E-03	
51	3,210.0	3,210.0	45.0	Sandstone	2,022	4.03E+06	0.302	0.0	0.00	0.00	1.0000E-02	5.1247E-04	✓
52	3,255.0	3,255.0	10.0	Dolomite	2,050	4.86E+06	0.321	0.0	0.00	0.00	1.0000E-02	5.1247E-04	
53	3,265.0	3,265.0	35.0	Sandstone	2,271	4.47E+06	0.340	0.0	0.00	0.00	1.0000E-02	5.1247E-04	✓
54	3,300.0	3,300.0	10.0	Dolomite	2,192	4.59E+06	0.324	0.0	0.00	0.00	0.0000E+00	0.0000E+00	
55	3,310.0	3,310.0	10.0	Dolomite	2,287	4.29E+06	0.331	0.0	0.00	0.00	0.0000E+00	0.0000E+00	
56	3,320.0	3,320.0	20.0	Dolomite	2,194	4.32E+06	0.309	0.0	0.00	0.00	0.0000E+00	0.0000E+00	
57	3,340.0	3,340.0	60.0	Sandstone	2,155	5.70E+06	0.318	0.0	0.00	0.00	0.0000E+00	0.0000E+00	✓
58	3,400.0	3,400.0	50.0	Dolomite	2,489	4.92E+06	0.359	0.0	0.00	0.00	0.0000E+00	0.0000E+00	
59	3,450.0	3,450.0	50.0	Dolomite	2,267	4.67E+06	0.314	0.0	0.00	0.00	0.0000E+00	0.0000E+00	
60	3,500.0	3,500.0	50.0	Limestone	2,316	4.17E+06	0.304	0.0	0.00	0.00	0.0000E+00	0.0000E+00	
61	3,550.0	3,550.0	50.0	Dolomite	2,372	4.67E+06	0.321	0.0	0.00	0.00	0.0000E+00	0.0000E+00	
62	3,600.0	3,600.0	0.0	Limestone	2,484	4.61E+06	0.335	0.0	0.00	0.00	0.0000E+00	0.0000E+00	

Table 3
Stage 1 Pumping Schedule and Procedure

Stage	Volume, gal	Fluid	Conc.	Proppant
1 - Pre-pad	5,000	Proppant-consolidating treatment		
2 - Pad	15,000	Proppant-consolidating treatment		
3 - Sand-laden fluid	20,000	Proppant-consolidating treatment	1–3	Brown-12/20
4 - Sand-laden fluid	10,000	Proppant-consolidating treatment	3	Brown-12/20
5 - Sand-laden fluid	4,000	Proppant-consolidating treatment	3	* Brown-12/20
6 - Spacer	± 250	Proppant-consolidating treatment		
7 - Spot acid	1,000	15% Iron stabilizer		
8 - Flush	± 1,850	Proppant-consolidating treatment		

*Coat stage 5 with 1.5% proppant flowback-control fluid.

Table 4
Stage 2 Pumping Schedule and Procedure

Stage	Volume, gal	Fluid	Conc.	Proppant
1 - Pre-pad	5,000	Proppant-consolidating treatment		
2 - Pad	20,000	Proppant-consolidating treatment		
3 - Sand-laden fluid	20,000	Proppant-consolidating treatment	1–3	Brown-12/20
4 - Sand-laden fluid	10,000	Proppant-consolidating treatment	3	Brown-12/20
5 - Sand-laden fluid	4,000	Proppant-consolidating treatment	3	* Brown-12/20
6 - Flush	± 2,600	Proppant-consolidating treatment		

*Coat stage 5 with 1.5% proppant flowback-control fluid.

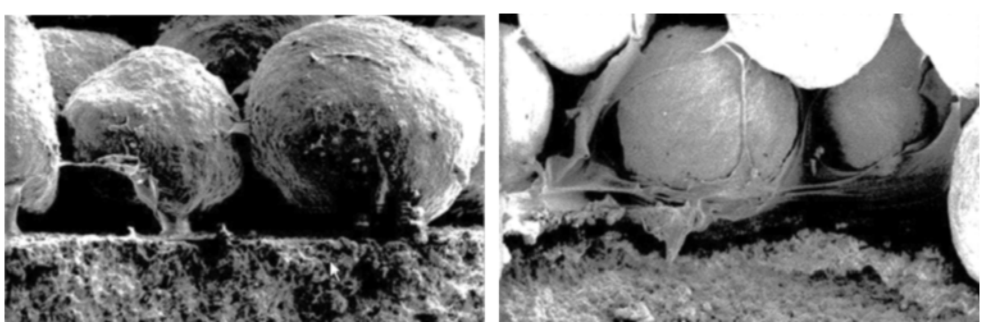

Figure 1—Photos Showing Guar in Fracture Pack (Proppant Pack) Porosity, or Damage

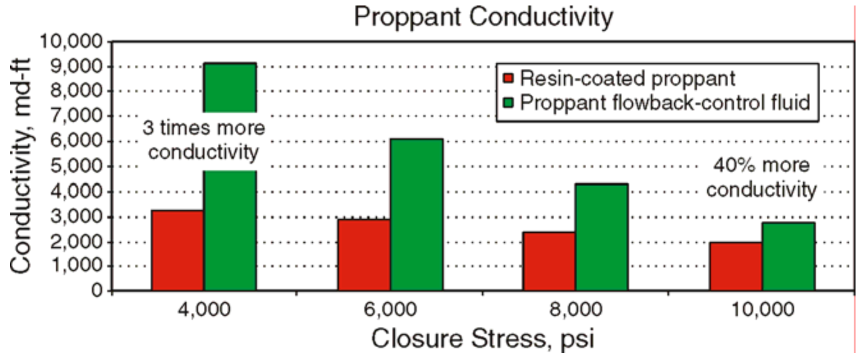

Figure 2—Conductivity Comparison Between RCP and New SMA Treatment
At 4,000-psi closure, the SMA treatment had 3 times more conductivity.
Even at 10,000 psi, there is 40% more conductivity with the new treatment.

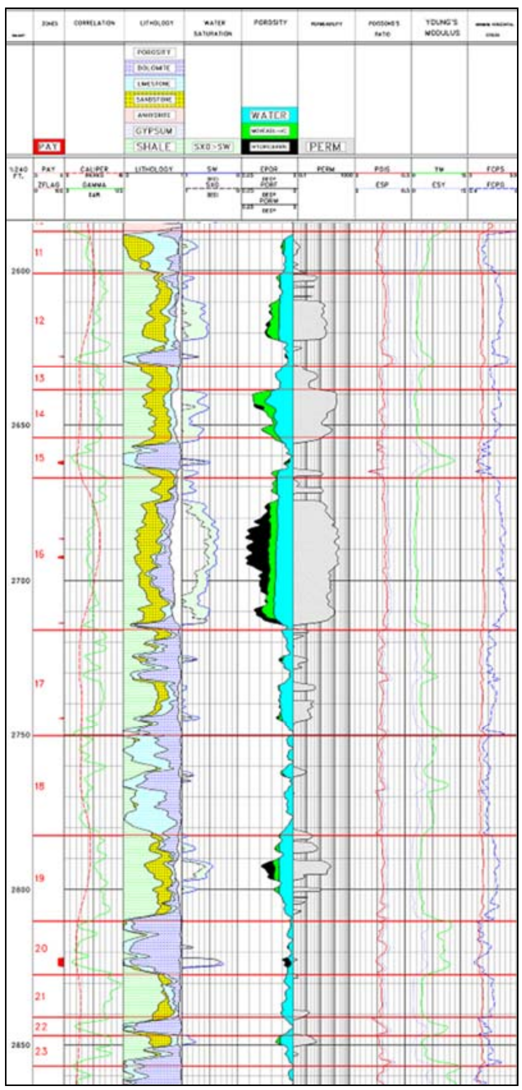

Figure 3—Frac log, Computed From Logging Inferences

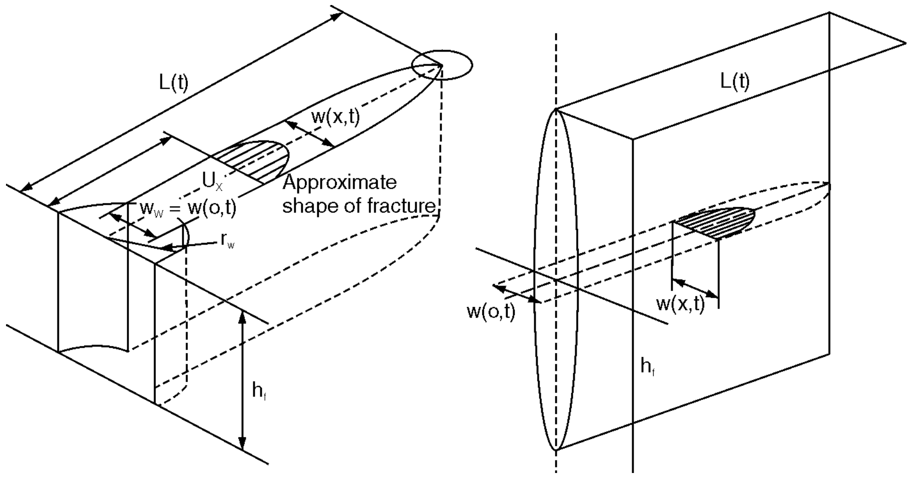

Figure 4—Early Fracture Model Geometry

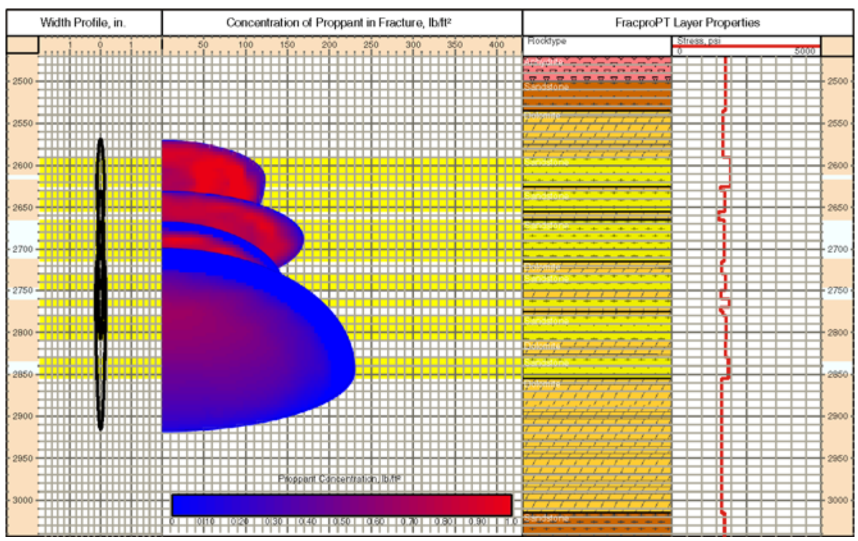

Figure 5—Fracture Profile with Logs and Layers for Well 1590, Yates Formation

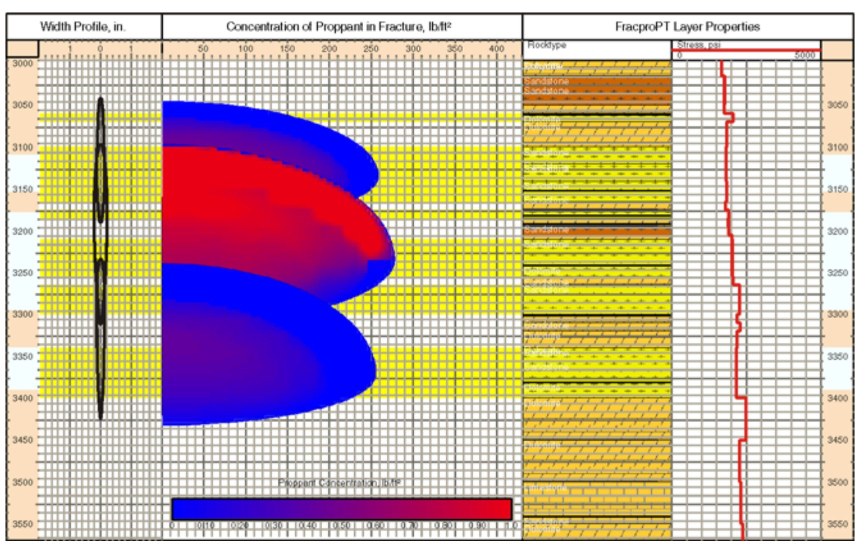

Figure 6—Fracture Profile with Logs and Layers for Well 1590, Queen Formation

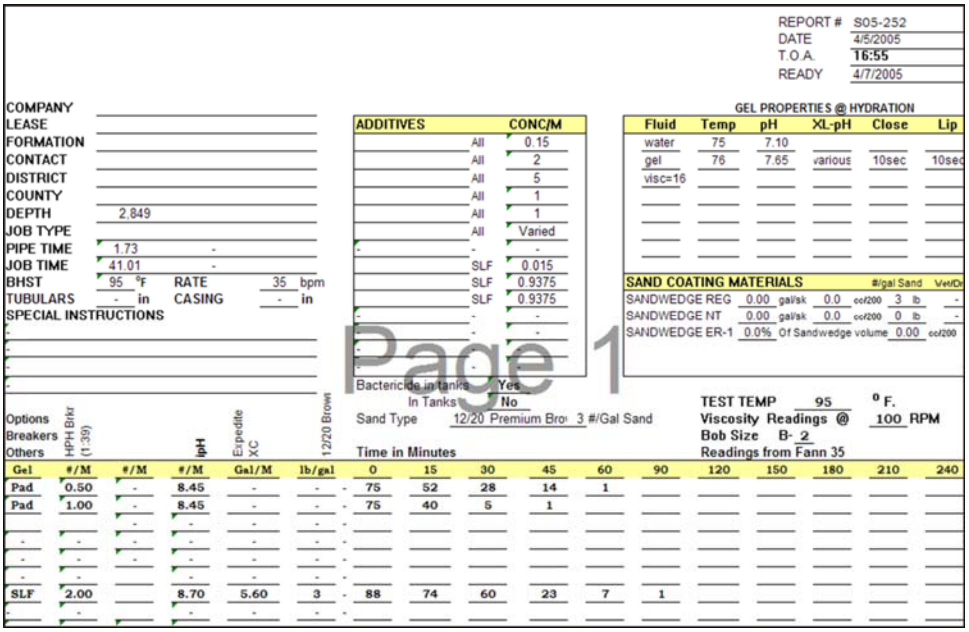

REPORT # S05-252
DATE 4/5/2005
T.O.A. 16:55
READY 4/7/2005

COMPANY
LEASE
FORMATION
CONTACT
DISTRICT
COUNTY
DEPTH 2,849
JOB TYPE
PIPE TIME 1.73 -
JOB TIME 41.01 -
BHST 95 °F RATE 35 bpm
TUBULARS - in CASING - in
SPECIAL INSTRUCTIONS

ADDITIVES		CONC/M
	All	0.15
	All	2
	All	5
	All	1
	All	1
	All	Varied
-	-	-
	SLF	0.015
	SLF	0.9375
	SLF	0.9375
-	-	-
-	-	-

Bactericide in tanks Yes
In Tanks No
Sand Type 12/20 Premium Bro 3 #/Gal Sand

GEL PROPERTIES @ HYDRATION

Fluid	Temp	pH	XL-pH	Close	Lip
water	75	7.10			
gel	76	7.65	various	10sec	10sec
visc=16					

SAND COATING MATERIALS #/gal Sand Vet/Dr

SANDWEDGE REG 0.00 gal/sk 0.0 cc/200 3 lb -
SANDWEDGE NT 0.00 gal/sk 0.0 cc/200 0 lb -
SANDWEDGE ER-1 0.0% Of Sandwedge volume 0.00 cc/200

TEST TEMP 95 °F.
Viscosity Readings @ 100 RPM
Bob Size B- 2
Readings from Fann 35

Options / Breakers / Others — HPH Brkr (1:39), pH, Expedite XC, 12/20 Brown; Time in Minutes

Gel	#/M	#/M	#/M	Gal/M	lb/gal	0	15	30	45	60	90	120	150	180	210	240
Pad	0.50	-	8.45	-	-	75	52	28	14	1						
Pad	1.00	-	8.45	-	-	75	40	5	1							
SLF	2.00		8.70	5.60	3	88	74	60	23	7	1					

Figure 7—Fluid Viscosity Reading, Break Data, Lab Results

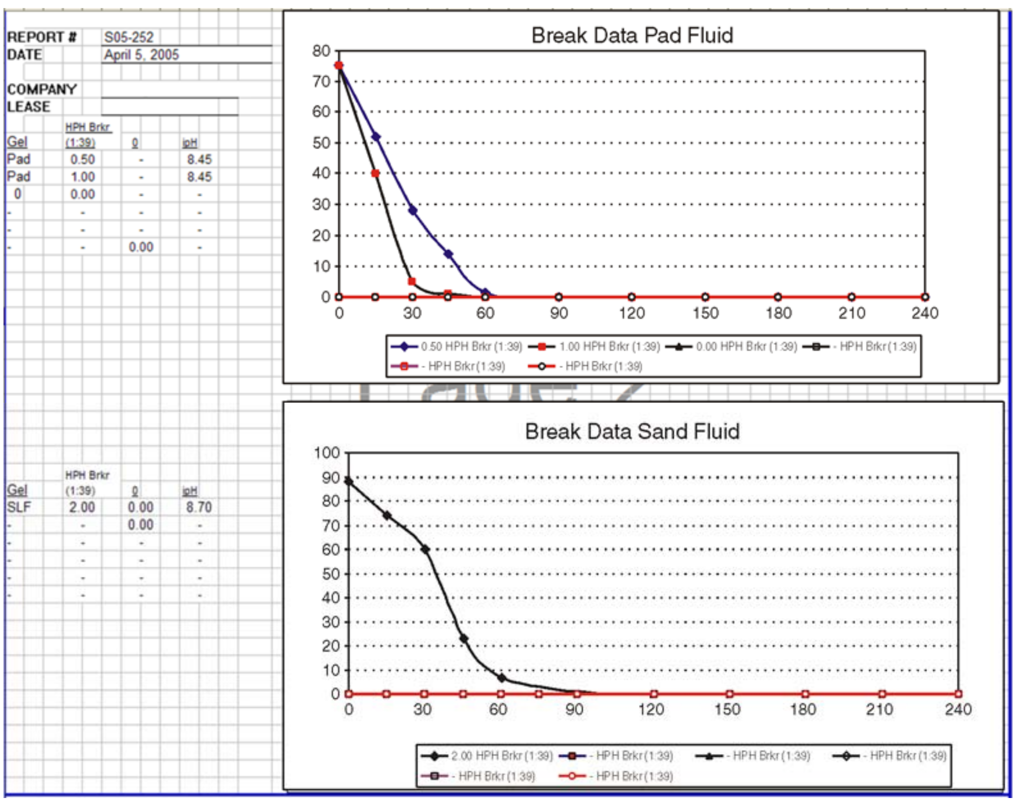

Figure 8—Break Character Curve, Lab Results

PERMIAN BASIN AREA LABORATORY
ODESSA, TEXAS

COMPANY		REPORT #	S05-252	DISTRICT	Odessa
Lease Well No.	GW O'Brien #1590	DATE	April 5, 2005	T.O.A	16:55
SUBMITTED BY		FLUID			

TANK #	32	182	237	304	910	912				
SP.GR.	1.000	1.000	1.000	1.000	1.000	1.000				
pH Water	6.45	6.55	7.05	7.15	7.15	7.15				
CHLORIDE	<500	<500	<500	<500	<500	<500				
SULFATES	200-400	200-400	200-400	200-400	200-400	200-400				
BICARBONATES	<300	<300	<300	<300	<300	<300				
SOLUBLE IRON	nil	nil	nil	nil	nil	nil				
QUATAMINES										
KCL IN WATER Y/N										

Figure 9—Water Analysis, Lab Results

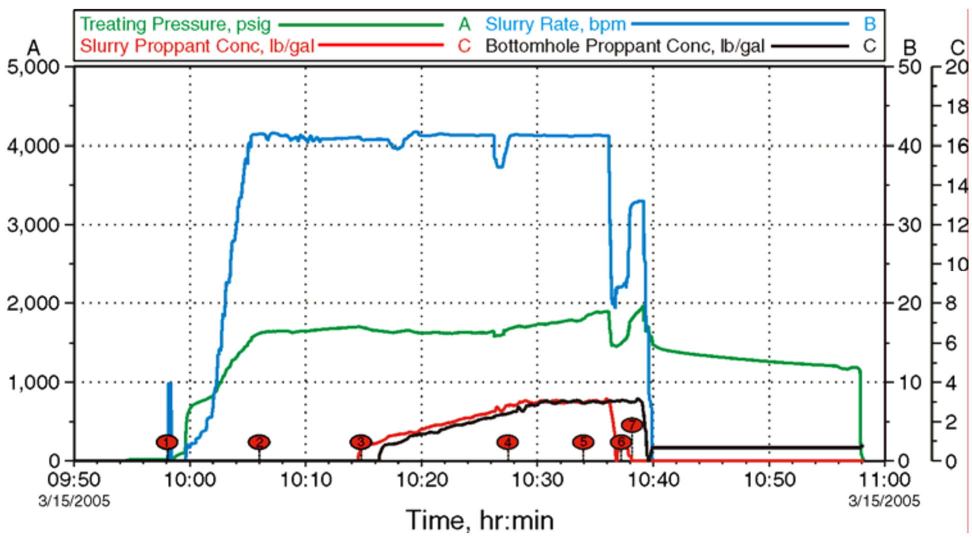

Figure 10—Treatment Data

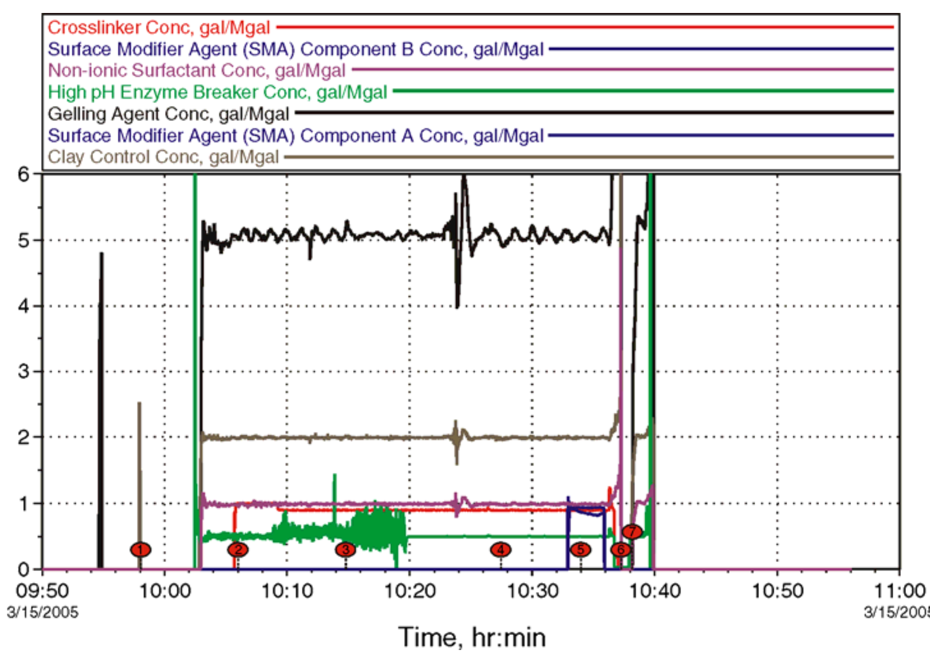

Figure 11—Additives Pumped

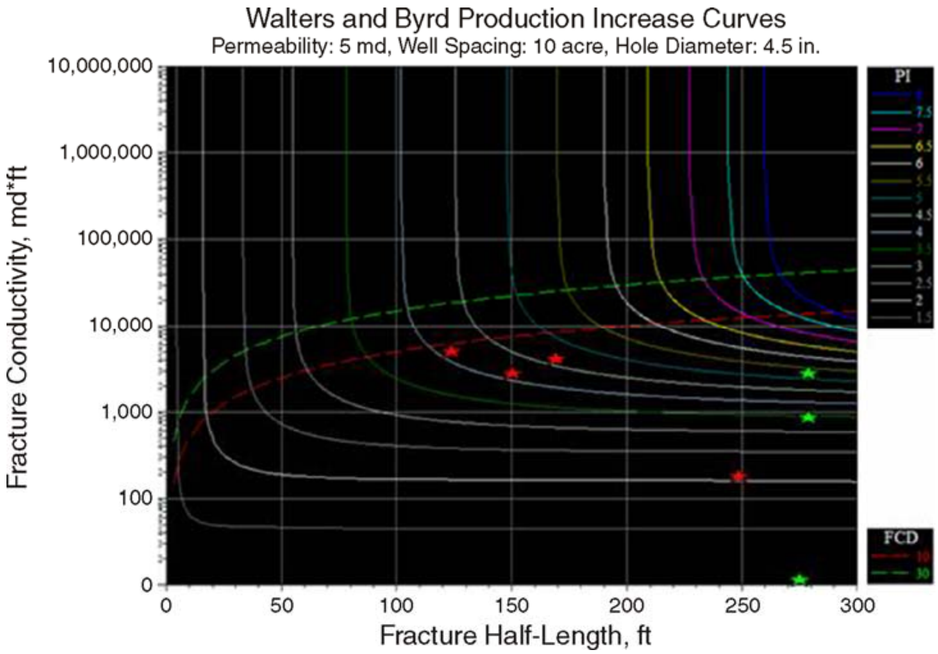

Figure 12—Walters and Byrd Folds-of-Increase Curves